Vol. 17(2), pp. 25-33, April-June 2024
DOI: 10.5897/JGRP2023.0864
Article Number:D29B58772155
ISSN 2070-1845

http://www.academicjournals.org/JGRP

ACADEMIC JOURNALS
expand your knowledge

Journal of Geography and Regional Planning

Full Length Research Paper

Sentinel-2 visible and near-infrared reflectance signature data for mapping potential geolocations of curb cuts in Hillsborough County, Florida

Heather McDonald[1]*, Namit Choudhari[2], Kayleigh Murray[1], Leomar White[1], Brooke Yost[1], Joseph Bohn[1] and Benjamin Jacob[1]

[1]College of Public Health, University of South Florida, Tampa, FL 33612 USA.
[2]School of Geosciences, University of South Florida, Tampa, FL 33620 USA.

Received 23 October, 2023; Accepted 26 April, 2024

A curb cut is a ramp that connects the sidewalk to a street crossing, thereby making it accessible for physically disabled pedestrians. Initially, ArcGIS Pro and machine learning algorithms in Python was utilized to classify a dataset of curb cut spectral signatures, leveraging Sentinel-2 imagery with a 10-m resolution. Initially, multispectral visible and near-infrared (NIR) Sentinel-2 sensors, along with machine learning geoprocessing tools in ArcGIS Pro, were utilized to generate signatures from curb cuts manually identified using Google Earth in Hillsborough County, Florida. Subsequently, we interpolated these capture points using a Python-modified Bayesian Maximum Likelihood Estimator to produce a cross-county signature map. The resulting layer was overlaid onto a zip-code gridded land use land cover (LULC) map and analyzed using a semi-parametric eigendecomposition eigen-spatial filtering approach. The hot/cold spot residuals represented independent curb cut clustering propensities. Utilizing higher sub-resolution satellite signals can optimize the identification of LULC classifiable, zip-code gridded capture point signatures, thereby improving the predictive mapping of other curb cut geolocations, such as those in school parking lots and homeless shelters. A real-time satellite mapping system can utilize sub-meter resolution data in a mobile application to retrieve a ranked list of visually similar curb cut geolocations.

Key words: Curb cuts, curb ramps, satellite data, ArcGIS, python, eigenvectors, Hillsborough County.

INTRODUCTION

A curb ramp, or curb cut, is a sloped transition that originates in the roadway and slopes upward through or builds up to a curbed pedestrian walkway, providing a smoother transition where the pedestrian walkway intersects with the roadway.

Curb ramps are a convenient sidewalk feature for many, making navigating the street easier for pedestrians encumbered by wheeled luggage, carts, and other rolling objects. However, their initial implementation by Jack Fisher, a lawyer and disabled veteran, in 1945 and their eventual revival in the 1970s by disabled students at the University of California at Berkeley occurred in the spirit

*Corresponding author. E-mail: hlmcdonald@usf.edu.

of ensuring greater accessibility for those with disabilities (Brown, 1999; Meldon, 2019). Despite America's prolific disability rights movement, which began in the 1960s and resulted in the passage of over fifty landmark pieces of legislation safeguarding the rights of disabled citizens, the inaccessible built environment of times before continues to set an inequitable precedent (Meldon, 2019). Although the implementation of curb cuts is widely regarded as one of the most successful implementations of universal design to date, significant gaps remain in implementation. The sporadic and sometimes bizarre placement of curb cuts continues to plague the lives of disabled pedestrians, serving to impede inter-community mobility and safety (Meyers et al., 2002). This calls for built environment solutions, which could be advised by a geographical information systems (GIS)-based needs assessment capable of identifying and mapping existing curb cuts.

A review of the existing peer-reviewed literature revealed that automated methodology and GIS have been implemented in the identification of curb cuts in various ways using non-satellite imagery (Ai and Tsai, 2016; Adams et al., 2022; Hara et al., 2014). Much of this research has focused on assessing compliance with accessibility legislation enforced at the time of the research (Ai and Tsai, 2016). However, this approach limits the research scope to compliance with specific laws, as interpreted by the researchers, rather than genuinely ensuring equitable access to pedestrian infrastructure.

Curb ramps have been successfully identified using semi-automated methodology with streetscape imagery such as Google Street View (GSV) (Adams et al., 2022; Hara et al., 2014). LIDAR has shown that the unique dimensional properties of curb ramps, in juxtaposition with the road and sidewalk, can be used to correctly classify them (Ai and Tsai, 2016). While effective for assessing sidewalk conditions, the machine learning and algorithmic GIS methodologies mentioned earlier are impractical for large counties and municipalities with extensive sidewalk networks, such as Hillsborough County. This is because street-level imagery does not constitute a field approach to inventory, relying on datasets obtained at a street-level scale via manual methods (that is, equipment necessitating travel along the entirety of the sidewalk network for data collection). Additionally, this methodological constraint means that the imagery is collected at inconsistent times, potentially missing alterations in the landscape, such as curb cut construction and degradation.

For these reasons, we depart from this methodology and utilize satellite imagery, which avoids introducing temporal inconsistency and error entirely.

Currently, there is no peer-reviewed literature on the use of satellite data for identifying curb cuts, likely due to the resolution limitations of other mediums and the small size of curb ramps. However, curb cuts possess spectrally unique, readily identifiable, and uniform characteristics that theoretically allow for sub-pixel eigenvector classification, particularly in the form of their detectable warning strips for the blind and visually impaired. In this experiment, Eigenvector Spatial Filter (ESF) forecast signature modeling was implemented to assess the geospatial locations of preexisting curb cuts.

Eigen-spatial filtering incorporates spatial structure into the linear predictor of any Generalized Linear Model (GLM) using a linear combination of signature eigenvectors derived from a spatial connectivity matrix. Jacob et al. (2023) introduced ESF to address difficulties in estimating non-normal remote sensing probability models. ESF has also been extended to tackle problems of network autocorrelation (Chun, 2008), multi-level models (Hu et al., 2018; Park and Kim, 2014), spatially varying signature coefficients (Murakami et al., 2017), geo-spatiotemporal residual zero/non-zero autocorrelation (Jacob and Novak, 2014), and various issues in epidemiologic infectious disease modeling (Jacob et al., 2023; Griffith et al., 2019). A geo-spatiotemporal non-normality test could be employed to determine whether georeferenced curb cut capture points are drawn from a non-normally distributed population in semiparametric, non-frequentistic eigenvector eigen-geospace. In this experiment, ESF was utilized to separate spatially structured random components from both trend and random noise, leading to statistical signature modeling with more robust statistical inference and applicability for interpolatable spectral curb-cut signature visualization. This separation process involves generating eigenfunctions of the matrix version of the numerator of the Moran Coefficient. Moran eigenvector spatial filtering conceptual material was employed to demonstrate the statistical features for detecting stratified curb cuts in a scalable, county-level, capture point signature estimator determinant model. Furthermore, an empirical, prognosticative curb cut model, utilizing Moran eigenvector spatial filtering, was summarized to quantify uncertainty-oriented signature reflectance error due to violations of regression assumptions in semiparametric eigenvector eigen-geospace.

Therefore, the goals of this research are to (1) construct the signatures of georeferenced curb cut geolocations on a land use land cover (LULC) map, (2) interpolate the signatures using Python to locate unknown geolocations of curb cuts, (3) field verify identified geolocations of curb cuts, and (4) demonstrate the validity of this methodology for future use in equity research and policy assessment concerning curb cut placement. This paper aims to illustrate and highlight the use of specific GIS tools to spotlight these community infrastructure challenge points and provide a technical explanation of the tools' use and the results they can produce. This research concludes with a statement on the public health importance of addressing this urban design issue and the need for advocacy to raise the priority of addressing these

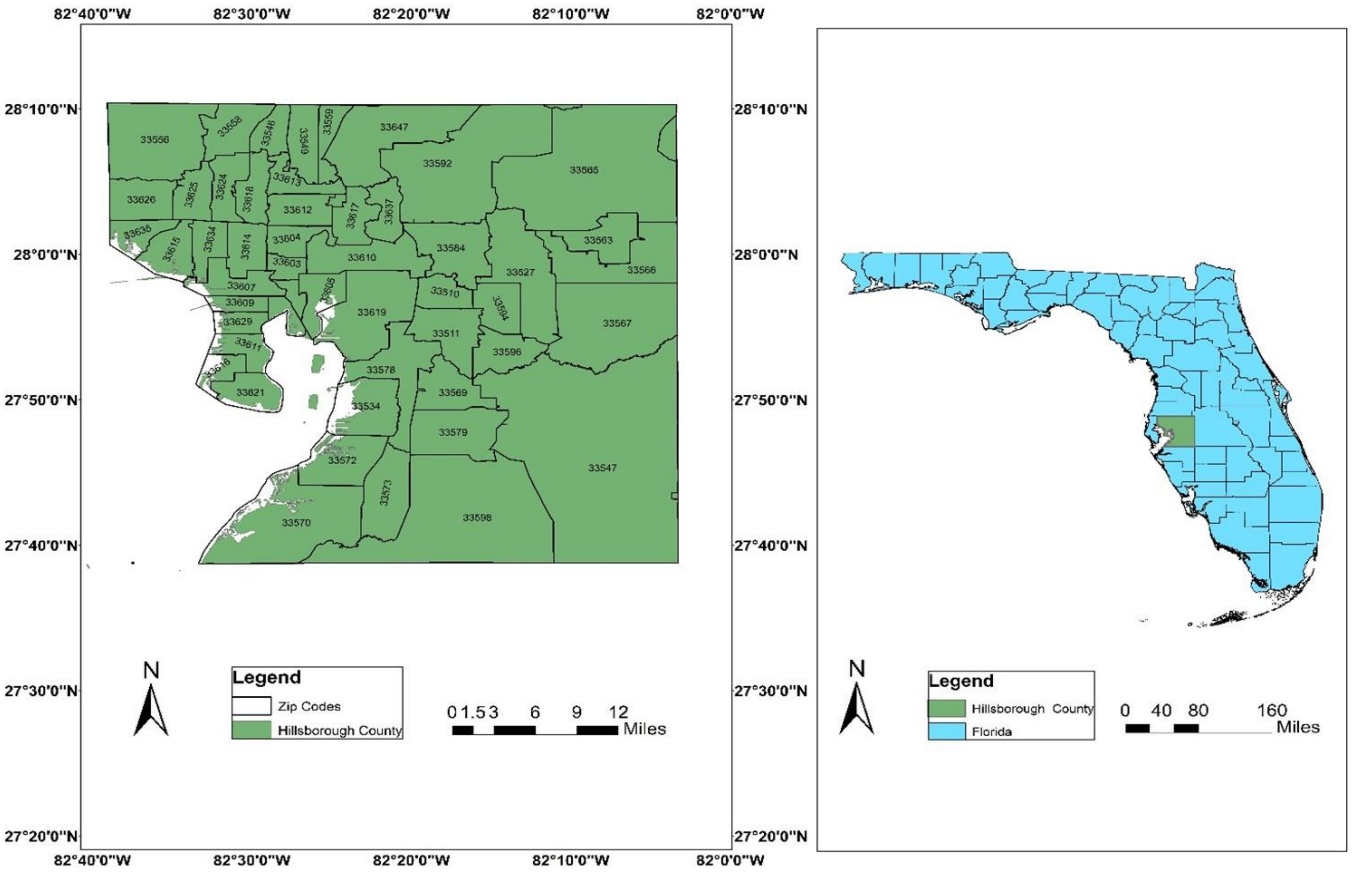

Figure 1. Study area map of Hillsborough County, Florida.
Source: Authors.

issues in this community and others.

METHODOLOGY

Study site

Hillsborough County, located in central Florida, is the fourth most populous county in Florida, with approximately 1.4 million residents (U.S. Census Bureau, 2021). It encompasses the cities of Tampa, Temple Terrace, and Plant City.

Hillsborough is part of the Tampa-St. Petersburg-Clearwater metropolitan area, which was ranked as the fourth most dangerous metropolitan area for pedestrians by the most recent 'Dangerous by Design' report (Smart Growth America, 2022). The county is responsible for maintaining over 3,200 linear miles of sidewalk (Hillsborough County, 2022). It is estimated that 11.6% of its residents have a reported disability, 6.5% have reported ambulatory difficulties, and 2.1% have reported vision impairments (U.S. Census Bureau, 2021) (Figure 1).

Signature determination

The European Space Agency's (ESA) high-resolution Sentinel-2B MSI (Multi-Spectral Instrument) Level-1C image from May 2023 was utilized to determine signatures of curb cuts. These curb cuts, equipped with compliant detectable warning mats within Hillsborough County's borders, were manually identified using Google Earth Pro software. The capture point candidates were further examined for condition and visually assessable indicators of ADA compliance using Google StreetView. Both the capture dates of satellite imagery and StreetView imagery were employed to temporally validate potential capture points. Due to the county's location between two swathes of Sentinel-2 imagery, equal representation between the North and South regions of the county was ensured within the final training sample.

Bayesian maximum likelihood classifier (MLC)

Maximum likelihood classification is a remote sensing classification technique that utilizes the Bayesian and Multivariate Gaussian Distribution (Stahler, 1980; Al-Ahmadi and Hames, 2009). It has a long history of use and remains popular in the field (Stahler, 1980; Maselli et al., 1992; Mingguo et al., 2009) (Figure 2). To determine if a pixel is part of a given class, the probability of the posterior can be used to define the likelihood of occurrence:

$$P(P_i|x) = \frac{P(P_i)P(x|P_i)}{P(x)}$$

where (Pi) is the probability of the i-th class, and $P(x)$ is the probability of a pixel. $P(x|P_i)$ can then be defined by:

$$P(P_i|x) = \frac{1}{\frac{n}{(2\pi)^2}|\Sigma_i|^{\frac{1}{2}}} ex\ p[-\frac{1}{2}(x-\mu_i)^T\Sigma_i^{-1}(x-\mu_i)]$$

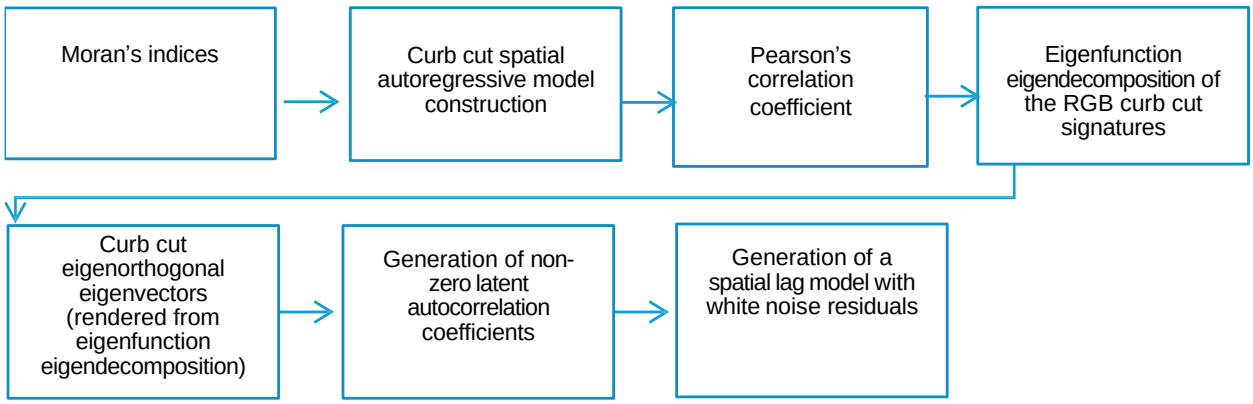

Figure 2. Summary of machine learning and spatial statistical pipeline.
Source: Authors.

where x is the feature vector of the pixel, $\mu i\mu$ is the mean vector of the i-th class features, Σi is the covariance matrix of the i-th class features, $^{\Sigma_i^{-1}}$ is the inverse covariance matrix of the i-th class features, and $||\Sigma i||$ is the determinant of the covariance matrix of the i-th class features.

This process can evaluate LULC and identify classes of interest using satellite imagery. The model constructed to apply this process to curb cuts defined six classes: agriculture, vegetation, water, infrastructure (buildings, etc.), roads, yellow curb cuts, and red curb cuts.

Spatial autocorrelation analyses

Autocorrelation indices employing the geosampled, georeferenced spectral estimator determinants were generated from the curb cut capture point data using Moran's indices (*I*). In simpler terms, it is a method to quantify the degree of spatial clustering of values in a 2-D space, commonly used used in geography and GIS to measure the clustering of unique features on a map, such as household income or level of education (Jensen, 2015). To calculate Moran's *I,* the following equation was used:

$$(N/W) * \Sigma\Sigma wij(xi - x)(xj - x)/\Sigma(xi - x)2$$

where N: the number of county units indexed by i and j, W: he sum of all wij, x: he variable of interest (spectral curb-cut signature, etc.), x: he mean of x, wij: A matrix of spatial weights.

It was assumed that the simple terms could quantify how closely the, curb-cut signature values were clustered together in a 2-D space. The upper and lower bounds for our eigen-decomposition model spatial matrix were constructible employing Moran's *I*, which here was given by"

$\lambda_{max}(n/1^TW\ 1)$ and $\lambda_{min}(n/1^TW\ 1)$,

where λ_{max} and λ_{min} were the extreme eigenvalues of Ω = HWH.

The components of each curb cut capture point's eigen-decomposed, eigen-orthogonalized eigenvector e_i, were subsequently mapped in ArcGIS Pro 2.8 onto an underlying geo-spatiotemporal discrete tessellation, which exhibited a distinctive topographic pattern ranging from positive spatial autocorrelation (PSA) (that is, similar values of log-transformed, count data clustering in eigenvector eigen-geospace) for $\gamma_i > E(I)$ to negative spatial autocorrelation (NSA) (that is, dissimilar log-values clustering in eigen-geospace) for $\gamma_i > E(I)$. Each geosampled, eigen-spatial filter, eigenvector estimator determinant was mapped where $E(I)$ was the expected value of Moran's *I* under the assumption of (a) spatial independence and (b) as outputs from related projection matrices $M_{(1)}$ or $M_{(X)}$, respectively.

Pearson's correlation coefficient

Moran's eigen-autocorrelation is an extension of Pearson's product-moment correlation coefficient (Griffith, 2003), denoted here as *I* to measure the extent of latent eigen-autocorrelation zero/non-zero coefficients in the eigen-spatial filter estimator-determinant covariate weights.Pearson's correlation coefficient was employed to summarize the autocovariance terms quantitated between the georeferenced eigenized estimator determinants. We calculated the covariance of the geosampled dataset of spectral curb cut covariates divided by the product of their standard deviations using:

$$\rho X, Y = \frac{\text{cov}(X,Y)}{\sigma_X \sigma_Y} = \frac{E[(X-\mu_X)(Y-\mu_Y)]}{\sigma_X \sigma_Y} \quad (1)$$

The formula defined the estimator determinant correlation coefficients.

Eigenfunction eigendecomposition of spectral signatures

The eigendecomposition eigen-spatial filtering approach added a minimally sufficient set of eigen-orthogonalized eigenvectors as proxy variables to the set of evidential, observational prognosticators in the model by inducing mutual independence in the geosampled signature estimator determinants within eigenvector eigen-geospace. The hot and cold spot residuals represented independent sentinel site clustering tendencies. The spatial pattern in the eigenvectors was synthetic. The predictive, positive, global eigen-autocorrelation in the local patterns of the curb cut signature parameters exhibited only positive local eigen-autocorrelation and vice versa for negative global eigen-autocorrelation. The eigenvectors e_i and e_j within each set of eigenvectors were mutually eigen-orthogonal employing symmetry transformation $\frac{1}{2}(V + V^T)$, which, in this experiment, was expressible when

Table 1. Confusion matrix of the maximum likelihood classification model based on the training data.

Parameter	Red curb cuts%	Yellow curb cuts%	Buildings%	Roads%	Vegetation%	Water%
Red curb cuts	91	0	0	1	0	15
Yellow curb cuts	0	90	9	4	1	0
Buildings	0	0	85	0	0	0
Roads	0	4	2	91	1	0
Vegetation	1	6	4	2	97	0
Water	8	0	0	2	1	85

Table 2. Confusion matrix of the maximum likelihood classification model based on random verification points.

Parameter	Red curb cuts%	Yellow curb cuts%
Red curb cuts	2	0
Yellow curb cuts	0	6
Buildings	0	26
Roads	0	54
Vegetation	90	14
Water	8	0

employing a quadratic form as revealed in Equation 1.

As mentioned previously, the eigen-spatial filter eigen-decomposed eigenvectors of specification were eigen-orthogonal to the geosampled, county-level X variable of the prognosticated, curb cut signature model constructed in Python employing the georeferenced estimator determinants.

Conversely, the eigenvectors of specification were eigen-orthogonal only to the constant unity vector 1 in X. This eigen-orthogonality had implications for predictive modeling geospatial misspecification terms in our stratifiable, signature, curb-cut related model, as they allow linking each collection of eigen-decomposed eigenvectors to its specific auto-regressed residuals by letting E_{SAR} be a matrix whose vectors are subsets of $\{e_1, \ldots, e_n\}_{SAR}$. Here, we also considered within-group estimation of higher-order, autoregressive, probabilistic panel models employing the georeferenced regressors and fixed effects where the lag order was potentially misspecified. Even when disregarding the misspecification bias, the fixed-effect bias formula regressed differently from the correctly specified case, though its asymptotic order remained the same under stationarity. A linear combination of this subset was approximated by employing the misspecification term of the simultaneous autoregressive version of the model output, which was expressible as:

$$(E_{SAR}\gamma \approx \sum_{k=1}^{\infty} \rho^k V^k \varepsilon) \quad (2)$$

The linear combination $E_{SAR}\gamma$ remained eigen-orthogonal to the geosampled exogenous variables X, so the estimated geosampled, stratified, curb cut signature-related predictor variables $\hat{\beta}$ were unbiased. Further, as a property of the ordinary least square (OLS) estimator, the approximated term $E_{SAR}\gamma$ was also eigen-orthogonal to the model residuals $\hat{\varepsilon}$. .

The model $y = X\hat{\beta} + E_{SAR}\hat{\gamma} + \hat{\varepsilon}$ decomposed the eigenized, stratified, prognosticative signature variable y into a systematic trend component, a stochastic signal component, and white-noise residuals. The term $E_{SAR}\hat{\gamma}$ removed variance inflation in the mean square error (MSE) term attributable to latent, non-zero eigen-autocorrelation embedded in the eigenized, curb cut signature-related estimator determinants.

Spatial lag model construction

For the spatial lag model (Equation 2), a georeferenced, predictive, curb cut signature-related model was constructible employing E_{Lag} , which was a matrix of those eigen-spatial filter, eigen-decomposed, eigenfunction eigenvectors that were a subset of $\{e_1, \ldots, e_n\}_{Lag}$. . The approximation of the misspecification term became $E_{Lag}\gamma \approx \sum_{k=0}^{\infty} \rho^k V^k (X\beta + \varepsilon)$. Since $E_{Lag}\gamma$ was correlated with the variables X, its incorporation into the scaled-up, capture point, county-level, stratified, curb cut signature-related model corrected the bias of estimated plain OLS parameters $\hat{\beta}$ in the latent, eigenized, spatial lag estimator determinant summary diagnostics. The model $y = X\hat{\beta} + E_{Lag}\hat{\gamma} + \hat{\varepsilon}$ was constructible from the geosampled, curb cut signature-related estimator determinants, which in this experiment were derivable from an eigendecomposition of the spatial lag model. However, for the georeferenced, eigenized estimator determinants, it was noted that the trend and the signals were no longer correlated, and the mean square error was deflated. Tables 1 and 2 show the confusion matrix of the maximum likelihood classification model based on the training data and random verification points.

RESULTS

Based on the training data for the MLC, the generated model displayed an overall accuracy of 80%, with a sensitivity of 91% and a specificity of 90%. Notably, the

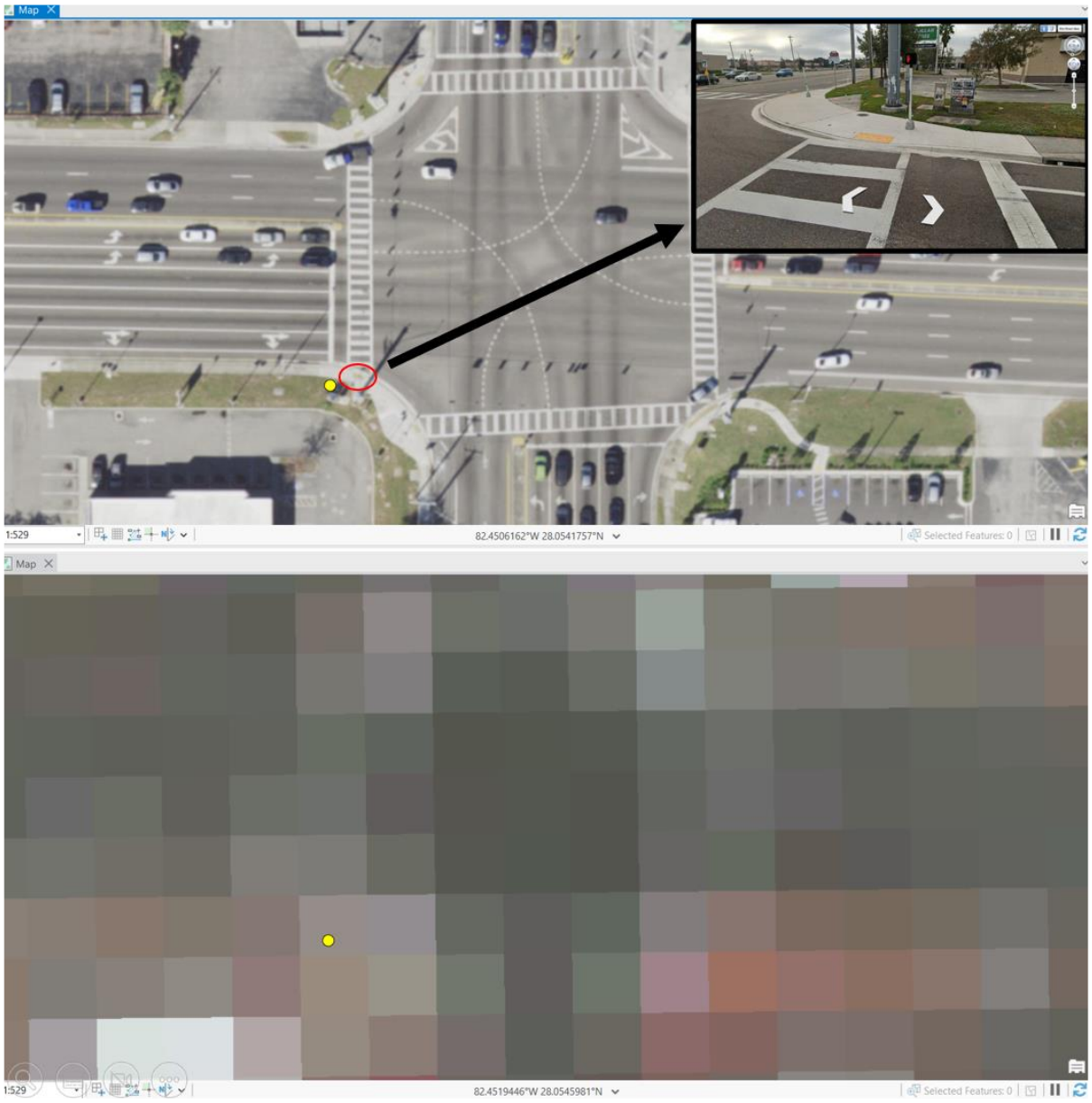

Figure 3. Predicted yellow curb cut from the maximum likelihood classification model.
Sources: Sentinel-2, ArcGIS Pro Imagery Basemap, and Google Earth.

training data showed accuracies of 91% for the red curb cut class and 90% for the yellow curb cut class, with the most frequent misclassifications being roads, vegetation, and water classes.

Random verification points were generated to assess the accuracy of the model output for determining unidentified curb cut locations. These results differed significantly from the training dataset. When the random verification points were applied, the majority of the predicted red curb cuts were misclassified as the vegetation class, with only 2% correctly identified as red curb cuts. Similarly, for the yellow curb cuts, only 6% were correctly predicted to be yellow. curb cuts. Most of the predicted yellow curb cuts were roads (including sidewalks) (Figure 3).

It is worth noting that, despite the misclassification of many extraneous objects as curb cuts, every 'true' curb cut present within the randomly generated verification dataset was accurately classified. Higher-resolution imagery would enable a better ability to distinguish between red curb cuts and vegetation, as well as yellow curb cuts and roads (including sidewalks). However, clustering propensities could not be cartographically determined with assured statistical soundness due to the

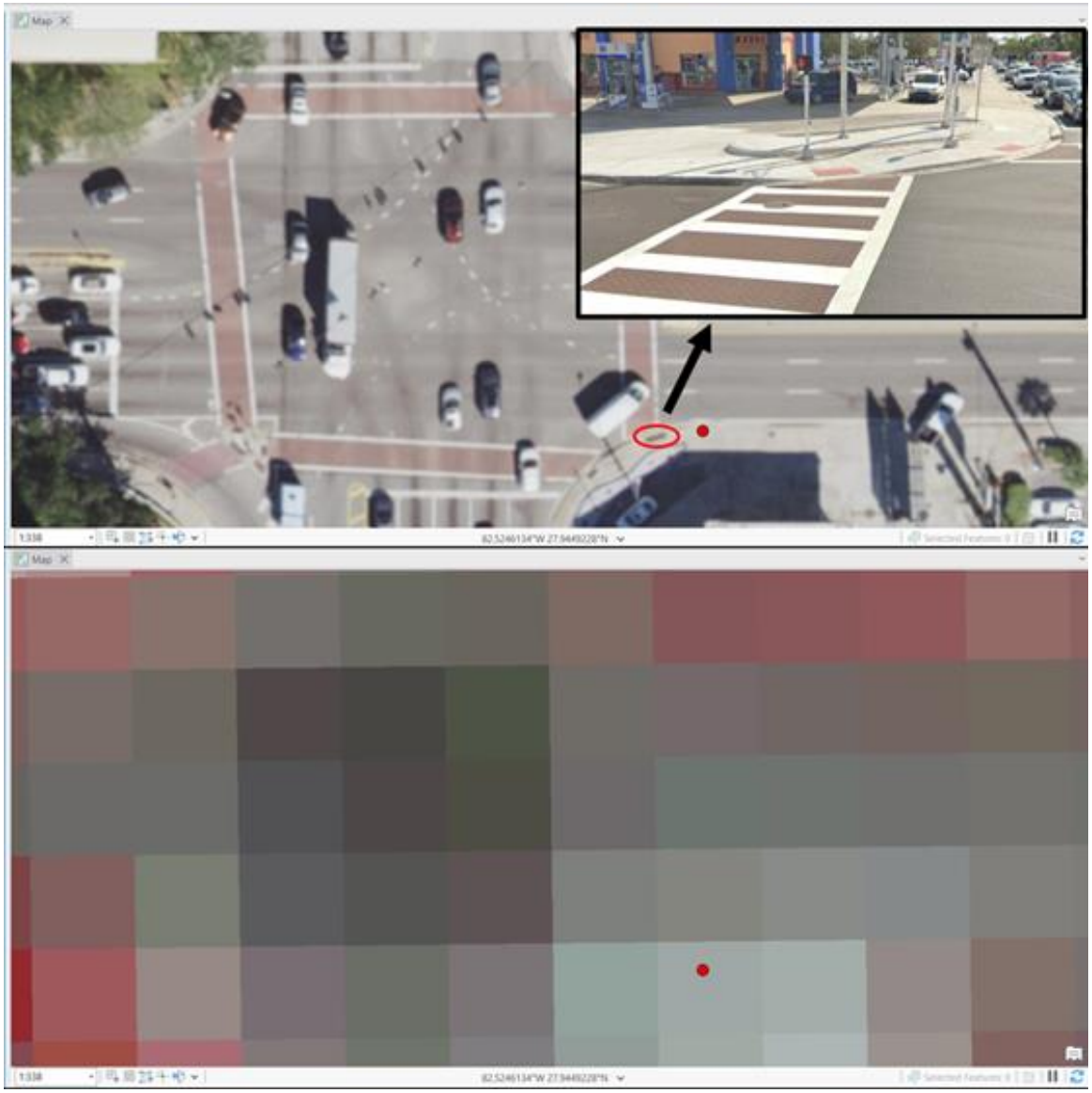

Figure 4. Predicted red curb cut from the maximum likelihood classification model.
Source: Sentinel-2, ArcGIS Pro Basemap Imagery, and Google Earth.

limited sample size of accurately interpolated curb cuts. This limitation directly stems from the resolution-related constraints imposed by the 10-m imagery (Figure 4).

DISCUSSION

This research indicates that curb cuts with detectable warning strips possess unique spectral reflectance characteristics that make them readily identifiable by automated classification methods, such as Python-modified maximum likelihood classification, on satellite imagery. Initially, we tested the scalability of the sentinel site using RGB curb-cut reflectance signatures from georeferenced capture points delineated using Google Earth to identify unknown curb cuts in the county.

This experiment introduced and evaluated a Bayesian Maximum Likelihood Estimation (BMLE) strategy to identify unknown sub-county curb cut geolocations. The BMLE did conduct spectral signature interpolation. Unfortunately, the spatial resolution of Sentinel-2 satellite data were limiting, as the signatures did not exceed 10 m. Discrepancies between training results and verification results were observed due to the necessity for sub-pixel classification, given the smaller size of detectable warning strips. With improved resolution, we hypothesize that the distinct pattern of the tactile dome mats will be visible and further distinguish these surfaces from similarly colored roadway paint and non-truncated curb ramps. Ideally, sub-meter resolution imagery would

enable more extensive discrimination of a sentinel site curb cut capture point, including conducting signature interpolation.

Regarding spatial analyses, a semi-parametric spatial filtering approach was employed to analyze spatial patterning. A subset of eigen-orthogonal eigen-spatial filter eigenvectors was derived from a transformed autocorrelation matrix. This was done with the intention of capturing the non-linear dependencies among the disturbances of the grid-stratified, autocorrelated data. However, it was found that an optimal residual subset within the curb cut-related signature forecast paradigm was more readily identifiable by an objective function that minimized erroneous non-zero autocorrelation rather than maximizing a diagnostic model fit. This function has the advantage of optimally quantifying deviance inclinations of spectrotemporal estimator determinants to ensure non-skewness, non-multicollinearity, and non-heteroscedasticity in curb cut signature forecasts. Violations of regression assumptions in eigenvector eigen-geospace can include unequal error variance and non-independence (Jacob, 2023). Employing smaller subsets of frugally selected, homoscedastic, non-multicollinear eigenfunction eigen-spatial filters can also reveal non-asymptoticalness in robust curb cut signature-dependent estimator determinants in eigenvector eigen-geospace. Once again, spectral resolution significantly hampered this analysis, but the methodology remains significant as it outlines a functional workflow for future analysis once a sufficient sample size is obtainable.

Community of interest and advocacy

For pedestrians with ambulatory and visual disabilities, curb cuts and truncated domes are not merely a matter of convenience or luxury; they are necessary for community integration, quality of life, and, in many cases, survival as a basic public health necessity in active transportation infrastructure for this population. Even a mere six-inch curb can present an insurmountable obstacle for wheeled mobility aid users and those with gait abnormalities. When a curb cut is absent or rendered unusable, individuals are forced to choose between backtracking to find an alternative route, abandoning their route altogether, or entering the roadway until another curb ramp is encountered. The U.S. Department of Justice (2020) recognizes curb ramps as one of the ADA's key issues and recommends detailed milestones for implementation within an entity's ADA Transition Plan. However, details are difficult to find within existing transition plans, and a lack of data collection detailing accessibility problems compounds this issue (Eisenberg et al., 2020).

Despite the potentially alarming role of inaccessibility in the perpetuation of financial and social inequities (Brumbaugh, 2018) as well as disparities in pedestrian casualties (Kraemer and Benton, 2015), enforcement of (the ADA often falls upon the groups most impacted by its shortcomings, and oftentimes, litigation is their chosen approach. The automated GIS data collection methodologies presented in this paper can allow municipalities to develop transition plans, apply for funding (State of Idaho, 2023), circumvent litigation, and ensure equitable pedestrian mobility and curb ramp access for all.

Conclusion

In this research effort, we determined that an ArcGIS/Python eigenfunction database interpolation model can forecast a Sentinel-2 imaged capture point sentinel site curb cut at the county level. Although this research was conducted at the county level, some implications may extend beyond Hillsborough County's borders. Many policy variables that contribute to the subject of study are not exclusive to Hillsborough County. As discussed, federal legislative shortcomings, such as those of the ADA, apply to the entire nation. Due to stringent definitions of curb cuts and the universality of truncated domes as a recognized form of detectable warning (Architectural and Transportation Barriers Compliance Board, 2023), this model has the potential for use across the United States. If a refined version of this model is applied across a varied set of municipalities and geographic boundaries, the geo-characteristics, population density, disability prevalence, and policies of these entities can be compared with the degree of curb cut implementation. New variables affecting municipalities' ability to provide curb cuts can be identified and addressed more precisely using higher resolution spatial imagery. Most importantly, municipalities can use high-resolution satellite data to advocate for grants and funding with accurate and detailed characterizations of their curb cuts and highly accurate cost estimation based on a robust dataset provided by our methodology.

CONFLICT OF INTERESTS

The authors have not declared any conflict of interests.

REFERENCES

Architectural and Transportation Barriers Compliance Board (2023). Accessibility Guidelines for Pedestrian Facilities in the Public Right-of-Way: A Rule by the Architectural and Transportation Barriers Compliance Board. Available at: https://www.federalregister.gov/documents/2023/08/08/2023-16149/accessibility-guidelines-for-pedestrian-facilities-in-the-public-right-of-way

Adams MA, Phillips CB, Patel A, Middel A (2022). Training computers to see the built environment related to physical activity: Detection of microscale walkability features using computer vision. International Journal of Environmental Research and Public Health 19(8):4548.

Ai CB, Tsai YC (2016). Automated sidewalk assessment method for Americans with Disabilities Act compliance using three-dimensional

mobile lidar. Transportation Research Record 2542:25-32.
Al-Ahmadi FS, Hames AS (2009). Comparison of four classification methods to extract land use and land cover from raw satellite images for some remote arid areas, Kingdom of Saudi Arabia. Journal of King Abdulaziz University, Earth Sciences 20(1):167-191.
Brown SE (1999). The curb ramps of Kalamazoo: discovering our unrecorded history. Disability Studies Quarterly 19(3):203-205.
Brumbaugh S (2018). Travel patterns of American adults with disabilities. Bureau Of Transportation Statistics, Washington DC, WA, USA, US Department of Transportation. Available at: https://www.bts.gov/sites/bts.dot.gov/files/2022-01/travel-patterns-american-adults-disabilities-updated-01-03-22.pdf
Chun Y (2008). Modeling network autocorrelation within migration flows by eigenvector spatial filtering. Journal of Geographical Systems 10(4):317-344.
Eisenberg Y, Heider A, Gould R, Jones R (2020). Are communities in the United States planning for pedestrians with disabilities? Findings from a systematic evaluation of local government barrier removal plans. Cities 102:102720.
Griffith DA (2003). Spatial autocorrelation and spatial filtering: Gaining understanding through theory and spatial vizualization. Springer.
Griffith DA, Chun Y, Li B (2019). Spatial regression analysis using eigenvector spatial filtering. Academic Press.
Hara K, Sun J, Moore R, Jacobs D, Froehlich J (2014). Tohme: detecting curb ramps in Google Street View using crowdsourcing, computer vision, and machine learning Proceedings of the 27th annual ACM symposium on User interface software and technology, Honolulu, Hawaii, USA. Available at: https://doi.org/10.1145/2642918.2647403
Hillsborough County (2022). Hillsborough approves an additional $20 million in sidewalk repair funding. Hillsborough County. Available at: https://www.hillsboroughcounty.org/en/newsroom/2022/05/04/hillsborough-approves-an-additional-$20-million-in-sidewalk-repair-funding
Hu Z, Hu H, Huang Y (2018). Association between nighttime artificial light pollution and sea turtle nest density along Florida coast: A geospatial study using VIIRS remote sensing data. Environmental Pollution 239:30-42.
Jacob BG, Izureta R, Bell J, Parikh J, Loum D, Casanova J, Gates T, Murray K, White L, Aceng JR (2023). Approximating Non-Asymptoticalness, Skew Heteroscedascity and Geo-spatiotemporal Multicollinearity in Posterior Probabilities in Bayesian Eigenvector Eigen-Geospace for Optimizing Hierarchical Diffusion-Oriented COVID-19 Random Effect Specifications Geo-sampled in Uganda. American Journal of Math and Statistics 13(1):1-43.
Jacob BG, Novak RJ (2014). Integrating a Trimble Recon X 400 MHz Intel PXA255 Xscale CPU mobile field data collection system using differentially corrected global positioning system technology and a real-time bidirectional platform within an ArcGIS cyberenvironment for implementing mosquito control. Advances in Remote Sensing, 3(3):141-196.
Kraemer JD, Benton CS (2015). Disparities in road crash mortality among pedestrians using wheelchairs in the USA: Results of a capture-recapture analysis. BMJ Open 5(11):e008396.
Maselli F, Conese C, Petkov L, Resti R (1992). Inclusion of prior probabilities derived from a nonparametric process into the maximum likelihood classifier. Photogrammetric Engineering and Remote Sensing 58(2):201-207.
Meldon P (2019). Disability history: The disability rights movement. National Parks Service. Available at: https://www.nps.gov/articles/disabilityhistoryrightsmovement.htm
Meyers AR, Anderson JJ, Miller DR, Shipp K, Hoenig H (2002). Barriers, facilitators, and access for wheelchair users: Substantive and methodologic lessons from a pilot study of environmental effects. Social Science and Medicine 55(8):1435-1446.
Mingguo Z, Qianguo C, Mingzhou Q (2009). The effect of prior probabilities in the maximum likelihood classification on individual classes: A theoretical reasoning and empirical testing. Photogrammetric Engineering and Remote Sensing 75(9):1109-1117.
Murakami D, Yoshida T, Seya H, Griffith DA, Yamagata Y (2017). A Moran coefficient-based mixed effects approach to investigate spatially varying relationships. Spatial Statistics 19:68-89.
Park YM, Kim Y (2014). A spatially filtered multilevel model to account for spatial dependency: application to self-rated health status in South Korea. International Journal of Health Geographics 13:6.
Smart Growth America (2022). Dangerous by Design 2022. Smart Growth America. Available at: https://smartgrowthamerica.org/dangerous-by-design/
Stahler AH (1980). The use of prior probabilities in maximum likelihood classification of remotely sensed data. Remote Sensing of Environment 10(2):135-163.
State of Idaho (2023). ADA curb ramp program. Idaho Transportation Department. Available at: https://itd.idaho.gov/alt-programs/
U.S. Census Bureau (2021). Disability characteristics. American Community Survey, ACS 5-Year Estimates Subject Tables, Table S1810. Available at: https://data.census.gov/table/ACSST5Y2021.S1810?q=disability+in+Hillsborough+County,+Florida
U.S. Department of Justice (2020). The ADA and city governments: Common problems. ADA.gov. Available at: https://www.ada.gov/resources/ada-city-governments/#issue-curb-ramps